

Understanding the Anomalously Long Duration Time of the Transmitted Pulse from a Soft Specimen in a Kolsky Bar Experiment

Hyunho Shin^{1#} and Jong-Bong Kim^{2,#}

¹ Mechanics of Materials Laboratory, Department of Materials Engineering, Gangneung-Wonju National University, 7 Jukheon-ghil, Gangneung, Gangwon-do, 25457, South Korea
² Computational Mechanics and Design Laboratory, Department of Mechanical and Automotive Engineering, Seoul National University of Science and Technology, 232 Gongneung-ro, Nowon-gu, Seoul, 01811, South Korea
 # Corresponding Author / E-mail: hshin@gwnu.ac.kr, TEL: +82-33-640-2484, FAX: +82-33-640-2244
 E-mail: jbkim@seoultech.ac.kr, TEL: +82-2-970-6434, FAX: +82-2-979-7032

KEYWORDS: Kolsky bar, Pulse duration time, Soft specimen, Transmitted signal

The reason for the observation of an anomalously long pulse duration time of a signal transmitted from a soft specimen in a Kolsky bar experiment is investigated. A systematic numerical experiment based on explicit finite element analysis has been carried out using elastic specimens with varying elastic moduli. The soft specimen is in a compressive state even after the passage of the pulse because it cannot push the bars, such that a fairly long transmitted pulse is monitored at the gage position of the output bar. The arrival of the second pulse (tensile) from the right-end surface of the output bar releases the first transmitted signal (compressive) coming from the compressed state of the specimen, which puts an end to the fairly long transmitted pulse. Because the observation of a prolonged transmitted pulse is a natural phenomenon, the prolonged transmitted pulse should not annoy researchers in the process of confirming the validity of experiments on soft specimens. Our concern in verifying the validity of experiments can be limited to other aspects such as the process of measurement and the amplification of weak transmitted signals coming from soft specimens.

Manuscript received: September 13, 2015 / Revised: November 12, 2015 / Accepted: November 14, 2015

1. Introduction

There has been high interest in high-strain-rate properties of solids.¹⁻³ The Kolsky bar (or split Hopkinson bar)⁴ has been used extensively to determine stress-strain curves of various materials at strain rates of 10^2 - 10^4 s⁻¹. Tested materials include metals, brittle solids (ceramics, rocks, and concretes),⁵ polymers,⁶ fiber-reinforced composites,⁷ and soft materials with only a few MPa's or less of strength like elastomers,^{8,9} foams,^{10,11} soils, skins, and viscous fluids. Not only compressive-mode Kolsky bars, but also tensile- and torsional mode Kolsky bars are available.^{12,13} As this study considers the compressive-mode Kolsky bar, Fig. 1 schematically illustrates the compressive-mode instrument.

Under the assumptions of 1D stress state, absence of inertia, and stress uniformity of the specimen, properties of the specimen are determined by the relationships:⁴

$$s(t) = (A_o/A)E_o e_T(t) \quad (1)$$

$$\dot{e}(t) = -2(C_o/L)e_R(t) \quad (2)$$

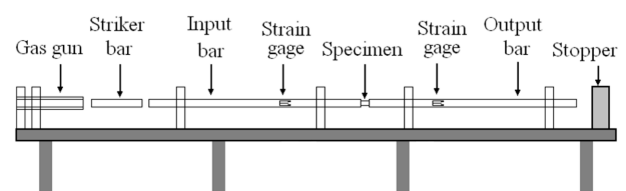


Fig. 1 Schematic illustration of a compressive-mode Kolsky bar

$$e(t) = -2(C_o/L) \int_0^t e_R(t) dt \quad (3)$$

In the above equations, s is the average (engineering) stress of the specimen, e is the average (engineering) strain of the specimen, \dot{e} is the rate of engineering strain of the specimen, t is the time, and e_R and e_T represent the 'reflected' and 'transmitted' pulse records in the input and output bars, respectively;¹⁴ A_o is the cross sectional area of the bar, C_o is the velocity of sound in the bars, and A and L are the initial area

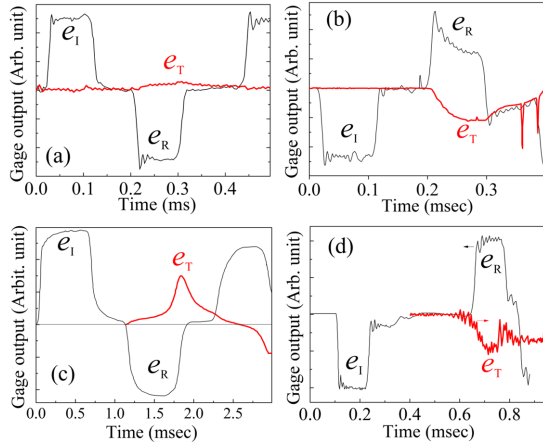


Fig. 2 Incident (e_i), reflected (e_R), and transmitted (e_T) pulse signal records from (a) a low density polyethylene (a tubular steel bar),⁶ (b) a polyurethane (an aluminum bar),¹¹ (c) an expanded polystyrene (a polymeric bar),¹⁰ and (d) a silicone rubber (an aluminum bar).⁹ Each diagram was reproduced by digitizing the data in the respective references

and the initial length of the specimen, respectively.

One of the important issues in testing soft materials using the Kolsky bar is that the magnitude of the transmitted signal e_T , which represents the stress of the soft specimen, is very small; a special type of signal processing (e.g., the amplification of only the e_T signal without amplifying the noise) is required to extract the weak e_T signal clearly from the noise. Use of a non-steel bar with a low elastic modulus material such as aluminum or magnesium assists in increasing the magnitude of the e_T signal, but e_T signals are still smaller than that from non-soft specimens in steel bars. When we use a polymeric bar, although the e_T signal is higher than it is for any other non-steel bars, the visco-elastic nature of the bar has to be additionally accounted for in the processing of the bar signal.

Another important issue in testing soft materials is that an anomalously long pulse duration time is generally observed in the transmitted e_T signal; Fig. 2 presents some examples found in experimental studies. As can be seen in Fig. 2, the pulse duration of the e_T signal is much longer than those of the e_i or e_R signals. Such behavior is never observed when non-soft specimens like metals and brittle materials are tested. Thus far, to our knowledge, no clear explanation for the appearance of an anomalously long duration of the e_T pulse from a soft specimen has been available in the literature. The poorly understood phenomenon of anomalously long pulse duration time of the e_T signal seriously annoys researchers in the process of verifying whether an experiment has been carried out reliably.

If the reason for the observation of an anomalously long pulse duration time of the transmitted signal (e_T) can be understood, efforts to ensure the reliability of Kolsky bar experiments for soft specimens can be limited to other aspects such as the process of measurement and the amplification of the weak e_T signal. Motivated by this reasoning, this study aims to elucidate why an anomalously long pulse duration time is observed in the transmitted signal (e_T). For this purpose, in this study, silicone rubber was selected as a representative soft material.

Table 1 Dimensions of the 3D long-bar system considered for numerical analysis and the number of 2D axi-symmetric elements to discretize half of the 3D space

	Diameter (mm)	Length (mm)	Number of elements (in half space)
Striker bar	20	250	2,500
Input bar	20	3,000	30,000
Specimen	10	3	441
Output bar	20	3,000	30,000

Table 2 Properties of materials for finite element analysis. ρ is the density, E is the elastic modulus, ν is the Poisson's ratio, and α and μ are the parameters of the Ogden model (N=1)

Notation	ρ (kg/m ³)	E (GPa)	ν	α	μ (MPa)	Remark
MS	7,850	210	0.35	-	-	Maraging steel (C350)
H	2,000	70-0.07	0.4	-	-	Hypothetical specimen
RB	970	-	0.5	2.5	8	Silicone rubber

Then, a systematic numerical experiment based on explicit finite element analysis was carried out using elastomeric specimens with varying elastic moduli.

2. Numerical Experiment

The dimensions of the considered Kolsky bar system are given in Table 1. The properties of the materials used for the numerical analysis are given in Table 2.

In the numerical experiment, the steel striker bar traveled at a constant velocity of 10 m/sec (a typical impact velocity for elastomeric materials); the impact was achieved at $t = 100 \mu\text{sec}$.

As comparison references to understand the complicated bar signals from rubber specimen, hypothetical specimens (noted as H in Table 2) with varying elastic moduli (70 GPa - 70 MPa) were considered. The values of the density and the Poisson's ratio of the hypothetical specimens given in Table 2 are intermediate between those of metals and rubbers. In order to describe the constitutive behavior of rubber, we employed the Ogden model¹⁵ for an incompressible, isotropic, and hyper-elastic solid. The one-term Ogden model describes the axial engineering stress (s) in terms of the stretch ratio $\lambda (= l/l_0$ where l is the length and l_0 is the initial length of the specimen) as

$$s = (2\mu/\alpha)[\lambda^{\alpha-1} - \lambda^{-1-\alpha/2}] \quad (4)$$

where α is the strain hardening exponent and μ denotes shear modulus under infinitesimal straining. The values of α and μ for silicone rubber⁴ were used here.

Considering the axi-symmetry of the Kolsky bar system, only half of the 3D space was discretized using four-node bilinear axi-symmetric quadrilateral elements. The number of elements in each discretized space is given in Table 1. The true stress values of 6 elements at the surface portion of the input and output bars, located at a distance of 1 m from the specimen, were monitored and their averaged (engineering) values at each bar (s_i , s_R , and s_T) are presented in this study.

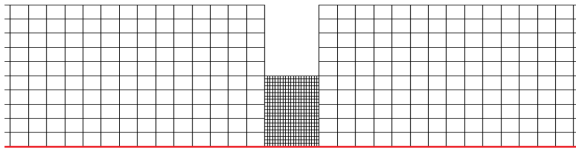


Fig. 3 Finite element meshes around the specimen. The bottom line (in red) is the axis of symmetry

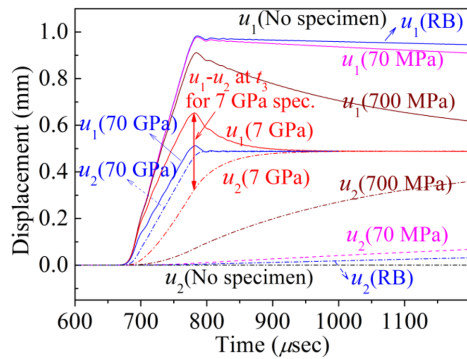


Fig. 4 u_1 and u_2 of elastic specimens with varying elastic moduli

The meshes around the specimen are shown in Fig. 3, which passed the mesh sensitivity test carried out separately. No friction was considered in this study while inertia was considered in the explicit analysis. A commercial finite element package, ABAQUS/Explicit,¹⁶ was used for the numerical analysis.

3. Data and Results

3.1 Displacement profile

The end surfaces of the input and output bars in contact with the specimen are noted by surfaces 1 and 2, respectively, and the displacement (velocity) of the respective surfaces are noted as u_1 (V_1) and u_2 (V_2). The values of u_1 and u_2 of all of the investigated specimens are compared in Fig. 4. Included in Fig. 4 is the case of no specimen ($E=0$); surface 1 is a free surface. As will be seen later in Fig. 5, the time when u_1 is maximized (t_3) is the moment when V_1 is zero, i.e., the passage of the pulse is finished at surface 1.

3.2 Velocity profile

The time derivatives of u_1 and u_2 , i.e., the velocities of surface 1 (V_1) and surface 2 (V_2) are presented in Fig. 5. In this figure, t_0 is the arrival time of the stress pulse at surface 1, t_1 is the time at which V_2 reaches V_1 , t_2 is the time after which V_1 (slope of u_1) is smaller than V_2 , and t_3 is the time at which V_1 is zero (this value varies from positive to negative). At t_3 , the passage of the pulse is over at surface 1 and also u_1 is at a maximum (Fig. 4). t_4 is the time at which V_1 is zero again (this value varies from negative to positive).

3.3 Stress profiles

The stress signals (s_T , s_R , and s_T) monitored in the bars are presented

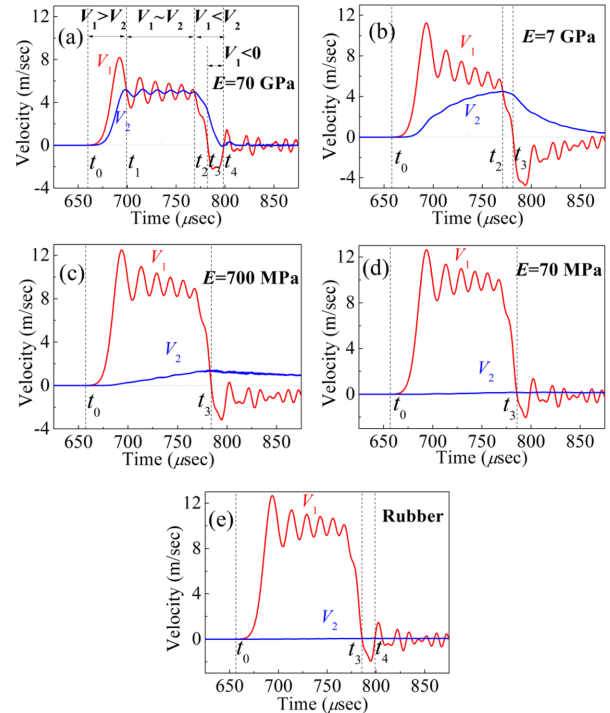


Fig. 5 V_1 and V_2 of elastic specimens with varying elastic moduli

in Fig. 6. Included in Fig. 6 are the *true* stresses of the specimen extracted from an element located near the center of the front surface of the specimen (σ_{sf}) and from one located at the back surface of the specimen (σ_{sb}). As can be seen in Fig. 6, the magnitude of the stress values (σ_{sf} and σ_{sb}) decreases notably as the elastic modulus of the specimen decreases. The magnitude of the s_T pulse, representing the stress of the specimen according to Eq. (1), is also the case. When the E value is very small, as is the cases of the 70 MPa specimen and the rubber specimen, the profiles of σ_{sf} , σ_{sb} , and s_T are very close to the baseline. For a clearer presentation of those profiles, their enlarged views are provided in Fig. 7.

4. Discussion

4.1 Prolonged duration of the transmitted pulse

For all of the investigated specimens in Fig. 4, at t_3 , u_1 is larger than u_2 , which means that specimens are in compressed states. The magnitude of u_1-u_2 at t_3 increases with the decrease of E , indicating that the compressive strain at t_3 increases with the decrease of E .

Another important aspect in Fig. 4 is that the value of u_1 decreases at $t > t_3$, which indicates that the specimen pushes back the input bar toward the striker side after the passage of the pulse. The increase of u_2 at $t > t_3$ indicates that the specimen also pushes the output bar to the stopper side (See Fig. 1). In overall, the magnitude of u_1-u_2 approaches zero as time increases from t_3 ; the compressed state of the specimen is released (The specimen is recovered). The recovery of the specimen is delayed with the decrease of E ; it takes longer time for a soft specimen to recover from the compressed state compared with a hard specimen.

The delayed recovery of the soft specimen is well monitored in the

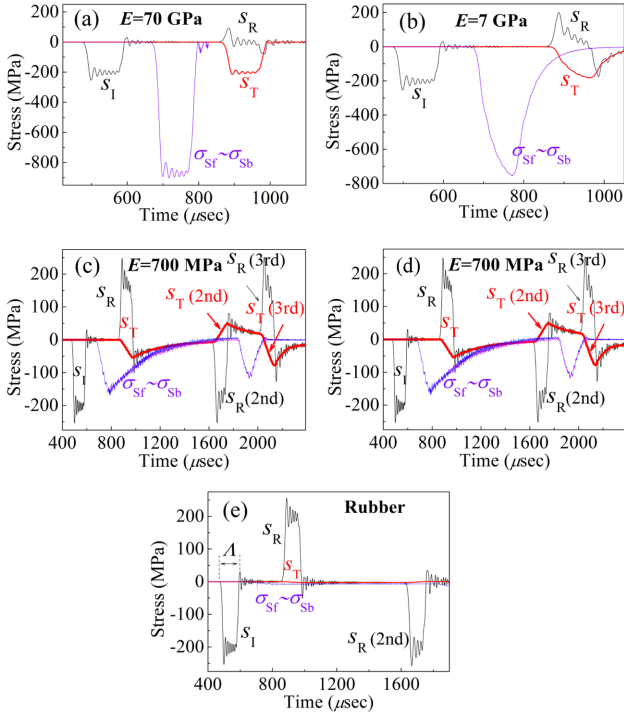


Fig. 6 Stress profiles of elastic specimens with varying elastic moduli

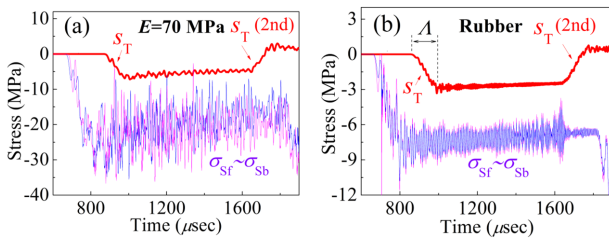


Fig. 7 Enlarged view of the stress profiles for (a) the specimen with an E value of 70 MPa and (b) the rubber specimen

bar signal (s_T) shown in Fig. 6. For the case of the specimen with an E value of 70 GPa (Fig. 6(a)), the compressive state of the specimen ($\sigma_s (= \sigma_{s_f} - \sigma_{s_b})$ profile) is released at approximately 796 μsec . This specimen pushes back the input bar and pushes the output bar soon after t_3 (796 μsec), as can be seen in Fig. 4. Compared with the 70 GPa specimen, the $\sigma_s (= \sigma_{s_f} - \sigma_{s_b})$ profile of the 7 GPa specimen (Fig. 6(b)) shows that it is in the compressed state for a prolonged time period (up to approximately 1000 μsec), which results from (is associated with) delayed recovery of the displacement at this time (approximately 1000 μsec ; Fig. 4). This prolonged compressive state of the 7 GPa specimen is well monitored in the prolonged s_T pulse that represents the specimen stress (Eq. (1)).

For the specimen with an E value of 700 MPa, recovery of the $\sigma_s (= \sigma_{s_f} - \sigma_{s_b})$ profile (the release of the compressed state) is even further delayed than the specimen with an E value of 7 GPa. The softer nature of this specimen ($E=700$ MPa) than the 7 GPa specimen is responsible for more prolonged recovery.

When the elastic modulus of the specimen is very low, e.g., in the

cases of the 70 MPa specimen and the rubber specimen, the specimen itself is incapable of recovering within the time period of the typical Kolsky bar experiment (approximately 1-2 msec) because the specimen is too soft to push back the input bar in the left direction and push the output bar in the right direction, as can be seen in displacement profiles (Fig. 4) and $\sigma_s (= \sigma_{s_f} - \sigma_{s_b})$ profiles (Fig. 6).

4.2 Termination of the transmitted pulse

In the $\sigma_s (= \sigma_{s_f} - \sigma_{s_b})$ profile of the 700 MPa specimen (Fig. 6(c)), the specimen is compressed first from approximately 674 μsec by the entrance of the stress pulse. It is compressed again from approximately 1834 μsec . This re-compression occurs because the former s_R pulse (tensile) returns from the left-end of the input bar in a compressed mode to compress the specimen again. This second s_R (compressive) pulse is monitored earlier in the input gage from approximately 1626 μsec and is noted as ' s_R (2nd)'.

In Fig. 6(c), the s_T signal is the transmitted pulse monitored at the output bar. The duration time of this compressive s_T signal is overly long, as mentioned, due to the compressed state of the specimen (σ_s profile). At the moment when the compressive s_T signal starts to be released from approximately 1655 μsec , the former s_T pulse arrives at the gage position of the output bar as a tensile pulse from the right-end surface of the output bar; this pulse is noted as ' s_T (2nd)' in Fig. 6(c). Therefore, the arrival of the second s_T pulse (tensile) at approximately 1655 μsec releases the original s_T signal (compressive) coming from the compressed state of the specimen, which puts an end to the fairly long s_T signal.

In the $\sigma_s (= \sigma_{s_f} - \sigma_{s_b})$ profiles of the specimens with an E value of 70 MPa and the rubber specimen (Fig. 7), recompression of the specimens starts approximately from 1843 and 1825 μsec , respectively, because of the arrival of the second s_R (Figs. 6(d) and 6(e), respectively) from the left end of the input bar. Before the arrival of the second s_R , the decrease in the magnitude of σ_s (the recovery of the specimen) is negligible after the first compression because of the very soft nature of the specimens.

As can be seen in Fig. 7, the termination of the transmitted signal (s_T) by the arrival of the second s_T pulse (tensile) from the right-end surface of the output bar also occurs for the 70 MPa specimen and the rubber specimen. The exact duration time of the transmitted pulse from a soft specimen depends on the instrument; it depends on the distance between the strain gage in the output bar and the right-end of the output bar.

When we extract the stress information of the soft (rubber) specimen from the e_T (s_T) signal based on Eq. (1), only the early part of the e_T (s_T) signal is used, as marked by the time interval Δ in Fig. 7(b). This time interval (Δ) is the same as the pulse period of the s_I (or s_R) signal (Fig. 6(e)). The rest (the prolonged portion) of the e_T (s_T) signal in Fig. 7(b) is not used for Eq. (1). Therefore, the prolonged e_T (s_T) signal does not influence the test results of the soft specimen; the prolonged e_T (s_T) portion is recorded from the compressed state of the specimen after the stress pulse finished to pass through the specimen.

Because we now know through this study that there is nothing wrong in observing a prolonged e_T signal in experiments for a soft specimen (it is a natural phenomenon), the prolonged e_T signal should not annoy researchers in the process of verifying the validity of

experiments on soft specimens. Our concern in verifying the validity of experiments can be limited to other aspects such as the process of measurement and the amplification of the weak e_T signal coming from the soft specimen.

4.3 Reflected pulse from an elastic specimen

In Fig. 6, the s_R pulse increases with the decrease of the value of E . This subsection explains the reason for this trend. The strain rate (engineering) of the specimen in the Kolsky bar can be described by⁴

$$\dot{\epsilon}(t) = de/dt = -[V_1(t) - V_2(t)]/L \quad (5)$$

According to Eq. (2), the reflected pulse signal e_R contains information on the strain rate of the specimen; the strain rate is governed by the magnitude of $V_1 - V_2$ according to Eq. (5). As can be seen in Fig. 5, the magnitude of V_2 decreases notably as the E value of the specimen decreases; the magnitude of $V_1 - V_2$ increases. Therefore, it is natural to observe an increased magnitude of the e_R pulse (the s_R pulse in Fig. 6) with the decrease of the E value.

5. Conclusions

The reason for the observation of an anomalously long pulse duration time of a transmitted signal from a soft specimen in a Kolsky bar experiment has been investigated. A systematic numerical experiment based on explicit finite element analysis was carried out using hypothetical elastic specimens with varying elastic moduli. The soft specimen is in a compressive state even after the stress pulse has passed through the specimen because the specimen cannot push the bars, such that a fairly long transmitted pulse is monitored at the gage position of the output bar. The arrival of the second pulse (tensile) from the right-end surface of the output bar releases the first transmitted signal (compressive) coming from the compressed state of the specimen, which puts an end to the fairly long transmitted pulse. Therefore, the exact duration of the transmitted pulse is dependent on the distance between the strain gage and the right-end surface of the output bar: it is instrument-dependent. Because the overly long pulse duration time of the transmitted signal from a soft specimen is a natural phenomenon (there was nothing wrong in the experiment), the prolonged transmitted pulse should not annoy researchers in the process of verifying the validity of experiments on soft specimen. Our concern for confirming the validity of experiments can be limited to other aspects such as the process of measurement and the amplification of weak transmitted signals coming from soft specimens.

ACKNOWLEDGMENT

This study was financially supported by the Mid-Career Researcher Program under contract No. 2015R1A2A2A01002454 through an NRF grant funded by the MEST. It was also equally financially supported by the Foundation Research Program under contract No. UD140050GD through an Agency for Defense Development grant funded by the DAPA.

REFERENCES

1. Lee, T. H., "Development of a Theoretical Model to Predict Cutting Forces for Hard Machining," *Int. J. Precis. Eng. Manuf.*, Vol. 12, No. 5, pp. 775-782, 2011.
2. Ahn, T.-K. and Kim, K. W., "Semi-Empirical Method to Estimate Dynamic Stiffness of Pre-Deformed Elastomers," *Int. J. Precis. Eng. Manuf.*, Vol. 13, No. 12, pp. 2259-2262, 2012.
3. Cho, J.-U., Kinloch, A., Blackman, B., Rodriguez, S., Cho, C.-D., and Lee, S.-K., "Fracture Behaviour of Adhesively-Bonded Composite Materials under Impact Loading," *Int. J. Precis. Eng. Manuf.*, Vol. 11, No. 1, pp. 89-95, 2010.
4. Kolsky, H., "An Investigation of the Mechanical Properties of Materials at Very High Rates of Loading," *Proceedings of the Physical Society, Section B*, Vol. 62, No. 11, pp. 676, 1949.
5. Shin, H. and Kim, J.-B., "Correction Functions to Determine the Stress State of a Flattened Disk Specimen in Diametral Testing with Reference to Analytical Solutions for Circular Specimens," *Int. J. Precis. Eng. Manuf.*, Vol. 16, No. 13, pp. 2699-2707, 2015.
6. Hughes, F., Prudom, A., and Swallowe, G., "The High Strain-Rate Behaviour of Three Molecular Weights of Polyethylene Examined with a Magnesium Alloy Split-Hopkinson Pressure Bar," *Polymer Testing*, Vol. 32, No. 5, pp. 827-834, 2013.
7. Yang, I. Y., Jeong, J. Y., and Kim, J. H., "Fracture Toughness of CFRP Laminated Plates according to Resin Content," *Int. J. Precis. Eng. Manuf.*, Vol. 11, No. 2, pp. 309-313, 2010.
8. Shergold, O. A., Fleck, N. A., and Radford, D., "The Uniaxial Stress Versus Strain Response of Pig Skin and Silicone Rubber at Low and High Strain Rates," *International Journal of Impact Engineering*, Vol. 32, No. 9, pp. 1384-1402, 2006.
9. Chen, W., Lu, F., Frew, D. J., and Forrestal, M. J., "Dynamic Compression Testing of Soft Materials," *Journal of Applied Mechanics*, Vol. 69, No. 3, pp. 214-223, 2002.
10. Ouellet, S., Cronin, D., and Worswick, M., "Compressive Response of Polymeric Foams Under Quasi-Static, Medium and High Strain Rate Conditions," *Polymer Testing*, Vol. 25, No. 6, pp. 731-743, 2006.
11. Bryson, J. A., "Impact Response of Polyurethane," M.Sc. Thesis, School of Mechanical and Materials Engineering, Washington State University, 2009.
12. Nemat-Nasser, S., Isaacs, J. B., and Starrett, J. E., "Hopkinson Techniques for Dynamic Recovery Experiments," *Proceedings of the Royal Society of London A: Mathematical, Physical and Engineering Sciences*, Vol. 435, pp. 371-391, 1991.
13. Yang, R., Zhang, H., Shen, L., Xu, Y., Bai, Y., and Dodd, B., "A Modified Split Hopkinson Torsional bar System for Correlated Study of τ - γ Relations, Shear Localization and Microstructural Evolution," *Philosophical Transactions of the Royal Society of London A: Mathematical, Physical and Engineering Sciences*, Vol.

- 372, DOI NO. 10.1098/rsta.2013.0208, 2014.
14. Shin, H., Lee, H., Kim, J. B., and Yoo, Y. H., "A Numerical Verification of the Reliability of a Split Hopkinson Pressure Bar with a Total Bar Length of 3m and a Diameter of 1 Inch," *Applied Mechanics and Materials*, Vols. 799-800, pp. 681-684, 2015.
 15. Ogden, R. W., "Large Deformation Isotropic Elasticity-on the Correlation of Theory and Experiment for Incompressible Rubberlike Solids," *Proceedings of the Royal Society of London A: Mathematical, Physical and Engineering Sciences*, Vol. 326, No. 1567, pp. 565-584, 1972.
 16. Dassault Systèmes, "Abaqus 6.13 Documentation," <http://129.97.46.200:2080/v6.13/> (Accessed 5 JAN 2016)